

# Hidden free energy released by explicit parity-time-symmetry breaking

Hong Qin,<sup>1,2,\*</sup> William Dorland,<sup>1,3,†</sup> and Ben Y. Israeli<sup>4,‡</sup>

<sup>1</sup>*Princeton Plasma Physics Laboratory,  
Princeton University, Princeton, NJ 08540, USA*

<sup>2</sup>*Department of Astrophysical Sciences,  
Princeton University, Princeton, NJ 08540, USA*

<sup>3</sup>*Department of Physics, University of Maryland, College Park, MD 20742, USA*

<sup>4</sup>*Department of Physics of Complex Systems,  
Weizmann Institute of Science, Rehovot, Israel*

## Abstract

It is shown that the familiar two-stream instability is the result of spontaneous parity-time (PT)-symmetry breaking in a conservative system, and more importantly, explicit PT-symmetry breaking by viscosity can destabilize the system in certain parameter regimes that are stable when viscosity vanishes. This reveals that complex systems may possess hidden free energies protected by PT-symmetry and viscosity, albeit dissipative, can expose the systems to these freed energies by breaking PT-symmetry explicitly. Such a process is accompanied by instability and total variation growth.

One important origin of the complexity associated with plasma dynamics is the interaction between different charged components in plasmas. The two-stream interaction between two charged components mediated by electromagnetic or electrostatic field have been identified and studied extensively for many applications and devices [1–9], including the classical Kelvin-Helmholtz instability and bump-on-tail instability as special cases. It is also used as a standard benchmark for numerical algorithms and theoretical methods. In the present study, we show that conservative two-stream interaction is parity-time (PT) symmetric and the familiar two-stream instability is driven by the spontaneous PT-symmetry breaking (see Fig. 1a). More importantly, we show that finite viscosity breaks PT-symmetry explicitly (see Fig. 1b), which can lead to instability in certain parameter regimes where the dynamics is otherwise stable when there is no explicit PT-symmetry breaking by viscosity.

The physics underpinning the instability triggered by viscosity through explicit PT-symmetry breaking is that PT symmetry imposes strong constraints on the dynamics of the system and only permits instability through spontaneous PT-symmetry breaking. When these dynamic constraints are removed by viscosity or other dissipative mechanism, the system becomes less “rigid” or more “slippery”, which can lead to instability in certain parameter regimes that are stable for conservative systems.

This interesting, if not surprising, effect of viscosity can be contrasted with the viscosity induced total variation non-increasing in simple systems, such as those governed by a scalar hyperbolic conservation law. The main difference is that the dynamics of two-stream interaction is more complex—containing more degrees of freedom. Dissipative effects, including viscosity and friction, explicitly breaks the constraints of PT-symmetry and exposes the dynamics to lower energy states, and the process of jumping to lower energy states is accom-

panied by instabilities and thus total variation growth. In comparison, simpler systems have no such hidden lower energy state and viscosity only leads to total variation non-increasing for field variables.

We start from the following one dimensional two-fluid equation system with viscosity,

$$\frac{\partial n_j}{\partial t} + \frac{\partial}{\partial z} (n_j v_j) = 0, \quad (1)$$

$$\frac{\partial v_j}{\partial t} + v_j \frac{\partial v_j}{\partial z} - \nu_j \frac{\partial^2 v_j}{\partial z^2} - \frac{q_j}{m_j} E + \frac{q_j}{n_j m_j} \frac{\partial p_j}{\partial z} = 0, \quad (2)$$

$$\frac{d}{dt} \left( \frac{p_j}{(m_j n_j)^{\gamma_j}} \right) = 0, \quad (3)$$

$$\frac{\partial E}{\partial z} - \sum_j 4\pi q_j n_j = 0. \quad (4)$$

Here,  $j = 1, 2$  is the index for species, and  $q_j$ ,  $m_j$ ,  $\gamma_j$ , and  $\nu_j$  are charge, mass, polytropic index, and viscosity for each species. Equations (1)-(3) govern the dynamics of density, velocity, and pressure for each species. The coupling between the two species is mediated by the electrostatic field self-consistently determined by the Poisson equation (3). The equilibrium  $(n_{j0}, v_{j0}, p_{j0}, E_0)$  is assumed to be homogeneous with differential equilibrium flow for both species in the  $z$ -direction, i.e.,  $v_{10} \neq v_{20}$ . There is no equilibrium electric field, i.e.,  $E_0 = 0$  with  $\sum_j q_j n_{j0} = 0$ . Consider a small perturbation of the density, velocity, pressure, and electrostatic field of the form

$$\tilde{n}_j, \tilde{v}_j, \tilde{p}_j, \tilde{E} \sim \exp(ikz - i\omega t). \quad (5)$$

The linear dynamics of the system can be cast into the form of Schrödinger's equation,

$$H\psi = \omega\psi, \quad (6)$$

$$H = \begin{pmatrix} v_{10} & 0 & 1 & 0 \\ 0 & v_{20} & 0 & 1 \\ \omega_1^2 + v_{t1}^2 & -\omega_1^2 & v_{10} - i\nu_1 & 0 \\ -\omega_2^2 & \omega_2^2 + v_{t2}^2 & 0 & v_{10} - i\nu_2 \end{pmatrix}, \quad (7)$$

$$\psi = (\tilde{n}_1, \tilde{n}_2, \tilde{v}_1, \tilde{v}_2)^T. \quad (8)$$

In deriving Eqs. (6)-(7), the Poisson equation (4) and energy equation (3) have been used as constraints to eliminate  $\tilde{E}$  and  $\tilde{p}_j$  in favor of  $\tilde{n}_j$ . All quantities are dimensionless. A characteristic velocity  $V$  has been chosen to normalized all velocity fields, and all frequencies

variables, including  $H$ , are normalized by  $kV$ . The density perturbation  $\tilde{n}_j$  is normalized by  $n_{j0}$ , and  $\nu_j$  is normalized by  $k/V$ ,  $\omega_j^2 = 4\pi n_{j0}q_j^2/m_j k^2 V^2$  is the normalized plasmas frequency squared, and  $v_{tj}^2 \equiv \gamma_j p_{j0}/m_j V^2$  is the normalized thermal velocity squared. The system is determined by 8 dimensionless parameters:  $(\nu_1, \nu_2, v_{t1}, v_{t2}, v_{10}, v_{20}, \omega_1, \omega_2)$ .

Equation (6) assumes the form of Schrödinger's equation, but the Hamiltonian  $H$  is certainly not Hermitian, which is typical in classical systems. One of the characteristics of non-Hermitian systems, such as symplectic [10, 11], pseudo-Hamiltonian [12–17], and PT symmetric [18–24] systems, is that they admit instabilities, i.e., eigen frequency  $\omega$  with  $\text{Im}(\omega) > 0$ . The dynamics of non-Hermitian systems is more complex. For the two-stream interaction, charting the stability diagram in the 8D parameter space can be challenging. A systematic approach for analyzing the parameter dependence of instabilities is afforded by PT-symmetry analysis [24–27]. Here we briefly summarize this method.

For a non-Hermitian Hamiltonian  $H$ , we may ask if it respects other symmetries of physical importance. One such symmetry is PT symmetry, originated from the Lorentz group, the homogeneous symmetry of flat spacetime. The  $PT$  transformation is a discrete element of the Lorentz group  $O(1, 3)$ , which as a topological manifold contains 4 disconnected components. In general, we expect that physics is invariant with respect to only one of the components—the proper orthochronous Lorentz group  $SO^+(1, 3)$ . The whole Lorentz group  $O(1, 3)$  is a semi-direct product of  $SO^+(1, 3)$  and the discrete subgroup  $\{1, \mathcal{P}, \mathcal{T}, \mathcal{PT}\}$ , i.e.,

$$O(1, 3) = SO^+(1, 3) \rtimes \{1, \mathcal{P}, \mathcal{T}, \mathcal{PT}\}, \quad (9)$$

where  $\mathcal{P} = \text{diag}(1, -1, -1, -1)$  and  $\mathcal{T} = \text{diag}(-1, 1, 1, 1)$ . Knowing that physics is not invariant with respect to  $\mathcal{P}$  transformation or  $\mathcal{T}$  transformation, we can ask a weaker question: Is physics invariant with respect to the  $\mathcal{PT}$  transformation [28]? Bender initiated the program to study the physics associated with  $\mathcal{PT}$  transformation [18–24]. It was found that for conservative classical systems, including those in neutral fluids and plasmas, PT symmetry can result from reversibility [24–27]. This finding is consistent with Bender's original characterization of PT-symmetry as a loss-grain balance between two coupled subsystems. A Hamiltonian  $H$  is called PT symmetric if it commute with a PT operator,

$$PTH - HPT = 0, \quad (10)$$

where  $T$  denote complex conjugate and  $P$  is a parity operator, i.e.,  $P^2 = I$ . Note that here we have generalized the  $\mathcal{P}$  element of the Lorentz group to an arbitrary parity operator. A PT

symmetric  $H$  must have a spectrum that is symmetric with respect to the real axis, i.e., for every unstable mode  $\omega_R + i\omega_I$  ( $\omega_I > 0$ ), there must exist a damped mode  $\omega_R - i\omega_I$ . This topological constraint in spectrum space stipulates that in order for a stable PT symmetric system to become unstable when the system parameters vary, the stable eigenmodes on the real axis must collide (resonate) first. It was recently proved [24] that this collision is precisely the Krein collision [14, 15, 17] in pseudo-Hermitian systems. This process is illustrated in Fig. 1a, and it is the only route for a PT symmetric system to become unstable. Krein collision is a necessary but not sufficient condition for instability. Only collision between a negative-action mode (denoted by blue in Fig. 1a) and a positive-action mode (denoted by red) will lead to instability. A stable eigenmode itself is invariant under PT transformation, but an unstable or damped eigenmode is not, even though the governing equations are always PT symmetric. Thus, the destabilization of the system via Krein collisions breaks PT symmetry spontaneously. Without considering their geometric properties, the locations in the parameter space where instabilities are triggered were previously called exception points or thresholds. In a PT symmetric system, a stable mode is not allowed to wonder off from the real axis to become unstable by itself. The route of destabilization illustrated in Fig. 1b is forbidden by PT symmetry.

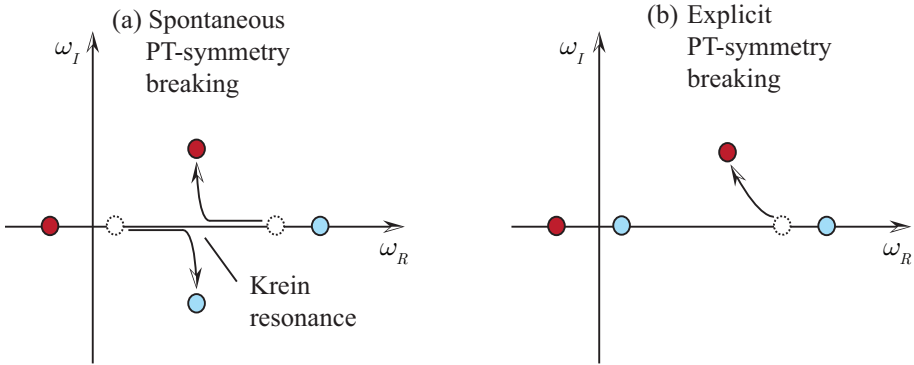


Figure 1. Spontaneous (a) and explicit (b) PT-symmetry breaking for a 4D system. Red and blue circles indicate positive- and negative-action modes, respectively. The route of destabilization illustrated in (b) is forbidden by PT symmetry.

However, if the PT-symmetry condition is explicitly broken, for example by a dissipative mechanism of viscosity or friction, then the constraint requiring spectrum being symmetric with respect to the real axis is removed, and the route to instability in Fig. 1b forbidden

by PT-symmetry is permitted. This is the mechanism of dissipation induced instability via explicit PT-symmetry breaking.

Instability driven by dissipation is an intriguing phenomena [29, 30]. In plasma physics, resistivity induced instabilities, including the tearing mode and the resistive-wall mode, belong to this category. Nevertheless, there exists an obvious question or doubt here: Dissipation always takes energy away from the system by definition; How can it drive the system more unstable? This issue has not been satisfactorily addressed in the literature. The physical picture presented here emphasizes the role of explicit PT-symmetry breaking by dissipation. A conservative system may possess lower energy states, but they are not accessible due to the PT-symmetry constraints. Dissipation explicitly breaks these constraints and expose the system to the lower energy states, albeit it may consume energy to do so. When the exposed energy drop dominates the dissipation, the system is destabilized.

Going back to the Hamiltonian specified by Eq. (7) for the two-stream interaction. When the viscosity  $\nu_1$  and  $\nu_2$  vanish, the system is trivially PT symmetric, for  $P = I$ . The spectrum is determined by the dispersion relation

$$\frac{\omega_1^2}{(\omega - v_{10})^2 - v_{t1}^2} + \frac{\omega_2^2}{(\omega - v_{20})^2 - v_{t2}^2} = 1. \quad (11)$$

As discussed above, the only route to instability is through the Krein collision between a positive-action mode and a negative-action mode [8]. When the instability is triggered, PT symmetry is spontaneously broken. Two numerically calculated examples are displayed in Figs. 2a and 2b for the case of mass ratio between two charge components being 100, and in Figs. 3a and 3b for the case of mass ratio being 1. Plotted in Figs. 2a and 3a are the imaginary parts of the 4 eigen-frequencies as functions of the relative equilibrium velocity  $\Delta v \equiv v_{20} - v_{10}$ . Figures 2b and 3b are the real parts of the eigen-frequencies. The system parameters in Figs. 2a and 2b are  $(\nu_1, \nu_2, v_{t1}, v_{t2}, v_{10}, v_{20}, \omega_1, \omega_2) = (0, 0, 0, 6, 0, \Delta v, 0.04, 4)$ . There are two Krein collisions in Fig. 2a at  $\Delta v = 2.44$  and  $\Delta v = 4.96$ , and the system is unstable for  $2.44 < \Delta v < 4.96$ . The system parameters in Figs. 3a and 3b are  $(\nu_1, \nu_2, v_{t1}, v_{t2}, v_{10}, v_{20}, \omega_1, \omega_2) = (0, 0, 1, 1, 0, \Delta v, 1, 1)$ . There are two Krein collisions in Fig. 3a at  $\Delta v = 2$  and  $\Delta v = 3.46$ , and the system is unstable for  $2 < \Delta v < 3.46$ . Observe that the spectrum in Figs. 2a and 3a is always symmetric with respect to the real axis, as required by PT symmetry.

For the  $H$  defined in Eq. (7), when the viscosity is non-vanishing, PT symmetry of the system is explicitly broken. It can be proven that there exist no parity operator  $P$  such

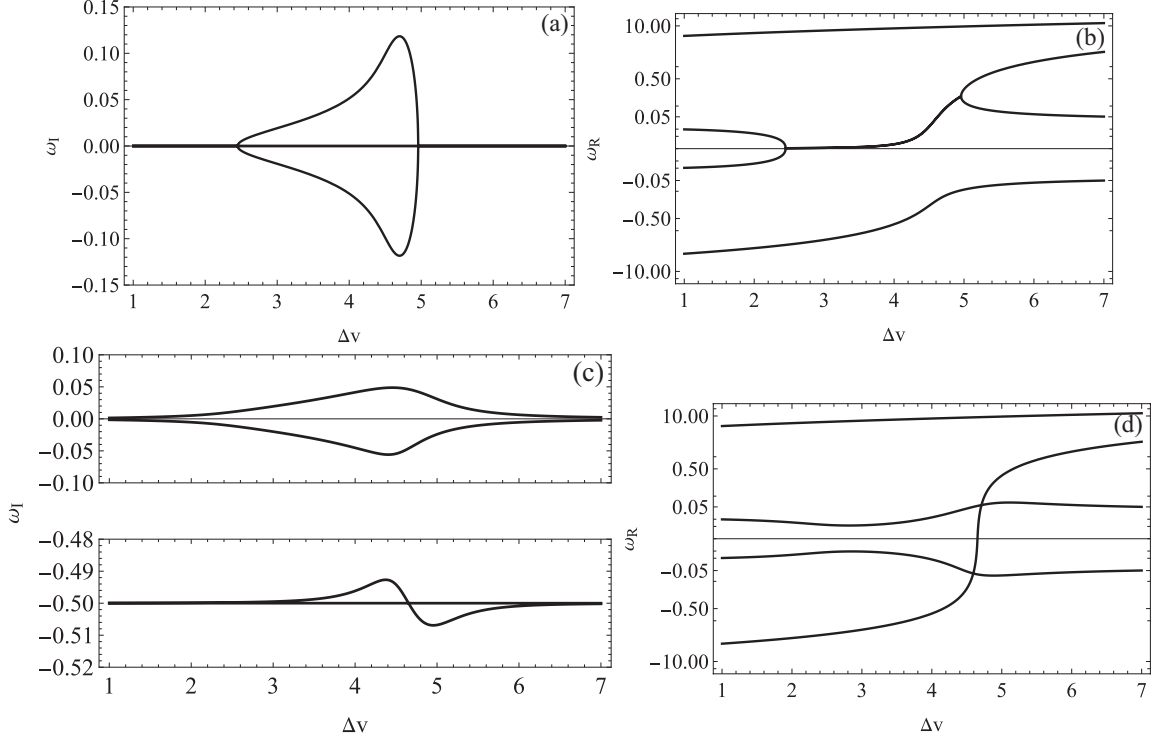


Figure 2. Two-stream instabilities for  $\omega_2/\omega_1 = 100$ . Plotted are the four eigen-frequencies  $\omega_R + i\omega_I$  of the system as functions of the differential velocity  $\Delta v$ . Absolute log scale was used for (b) and (d). The large empty space between  $-1.48 < \omega_I < -0.10$  is omitted in (c) for better resolution. The system parameters for (a) and (b) are  $(\nu_1, \nu_2, v_{t1}, v_{t2}, v_{10}, v_{20}, \omega_1, \omega_2) = (0, 0, 0, 6, 0, \Delta v, 0.04, 4)$ . There are two Krein collisions in (a) at  $\Delta v = 2.44$  and  $\Delta v = 4.96$ . The system parameters for (c) and (d) are  $(\nu_1, \nu_2, v_{t1}, v_{t2}, v_{10}, v_{20}, \omega_1, \omega_2) = (0, 1, 0, 6, 0, \Delta v, 0.04, 4)$ .

that  $PTH = HPT$ . Such cases are displayed in Figs. 2c, 2d, 3c, and 3d. The system parameters for Figs. 2c and 2d are  $(\nu_1, \nu_2, v_{t1}, v_{t2}, v_{10}, v_{20}, \omega_1, \omega_2) = (0, 1, 0, 6, 0, \Delta v, 0.04, 4)$ , which are identical to those for Figs. 2a and 2b except for the non-vanishing  $\nu_2$ . Because the governing system is not PT symmetric anymore, the spectrum is not symmetric with respect to the real axis and the route to instability illustrated in Fig. 1b is now possible. The system is unstable for entire plotted interval of  $1 < \Delta v < 7$ . In particular, the intervals  $1 < \Delta v < 2.44$  and  $4.96 < \Delta v < 7$  are stable regions when the viscosity vanishes. The two-stream instability in these two regions are triggered by the explicit PT-symmetry breaking induced by finite viscosity. A similar situation is found in Figs. 3c and 3d, where the system parameters are  $(\nu_1, \nu_2, v_{t1}, v_{t2}, v_{10}, v_{20}, \omega_1, \omega_2) = (0, 0.3, 1, 1, 0, \Delta v, 1, 1)$ , which are the same as those for Figs. 3a and 3b except for the non-vanishing  $\nu_2$ . Now the system is unstable for

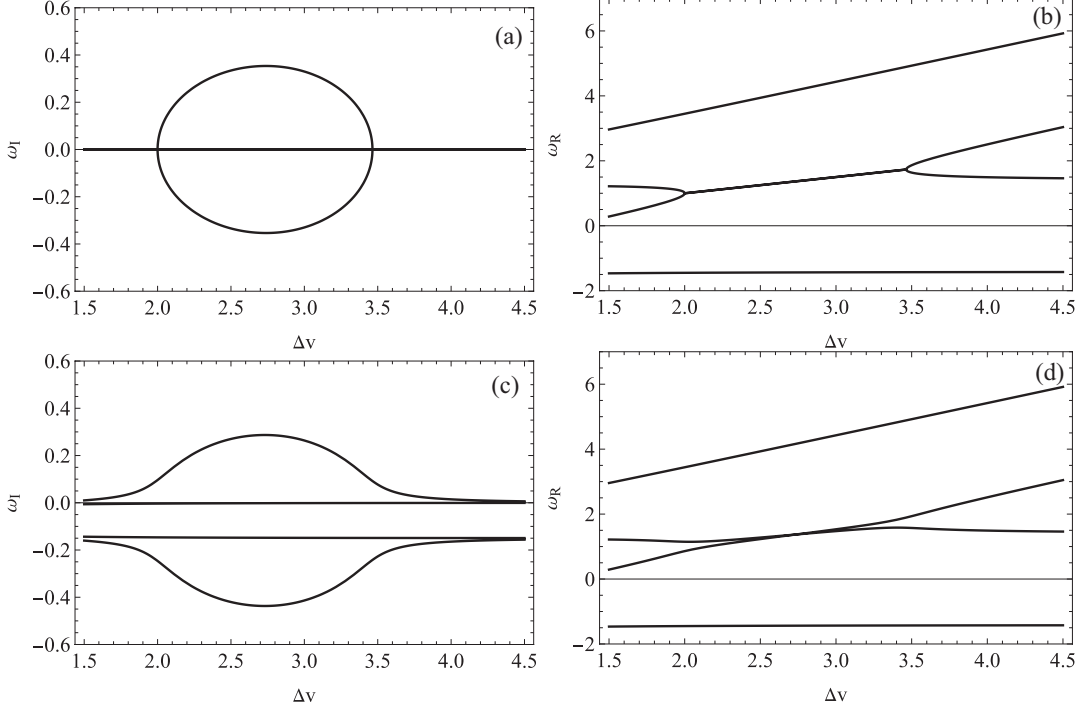


Figure 3. Two-stream instabilities for  $\omega_2/\omega_1 = 1$ . Plotted are the four eigen-frequencies  $\omega_R + i\omega_I$  of the system as functions of the differential velocity  $\Delta v$ . The system parameters for (a) and (b) are  $(\nu_1, \nu_2, v_{t1}, v_{t2}, v_{10}, v_{20}, \omega_1, \omega_2) = (0, 0, 1, 1, 0, \Delta v, 1, 1)$ . There are two Krein collisions in (a) at  $\Delta v = 2$  and  $\Delta v = 3.46$ . The system parameters for (c) and (d) are  $(\nu_1, \nu_2, v_{t1}, v_{t2}, v_{10}, v_{20}, \omega_1, \omega_2) = (0, 0.3, 1, 1, 0, \Delta v, 1, 1)$ .

the entire plotted interval of  $1.5 < \Delta v < 4.5$ , which includes two intervals,  $1.5 < \Delta v < 2$  and  $3.46 < \Delta v < 7$ , that are stable regions when there is no viscosity.

As discussed above, viscosity induced instability reveals that in addition to being an dissipative effect, viscosity can also reduce the rigidity of the dynamics and consequently inject free energy into the system. In the current context, the rigidity is represented by the PT-symmetry constraints of the conservative system. In general, complex system with large degrees of freedom is more likely to have this type of hidden free energy protected by the PT-symmetry constraints. The two-stream interaction described by Eqs. (1)-(4) is such a system. Specifically, the free energy is hidden in the differential equilibrium flow and pressure between the two components, as indicated in Eq. (11). In comparison, a scalar field  $u(t, z)$  governed by a hyperbolic conservation law

$$\frac{\partial u}{\partial t} + \frac{\partial}{\partial z} f(u) = 0 \quad (12)$$

does not have this type of free energy accessible by viscosity. Here,  $f(u)$  is a given function of  $u$ . In fact, the following result can rigorously proven [31]: Let  $\nu > 0$ , and  $u^\nu(t, z)$  is the solution of the following initial value problem,

$$\frac{\partial u^\nu}{\partial t} + \frac{\partial}{\partial z} f(u^\nu) = \nu \frac{\partial^2 u^\nu}{\partial z^2}, \quad (13)$$

$$u^\nu(t = 0, z) = u_0(z), \quad (14)$$

then the total variation of  $u^\nu$  defined by

$$\text{TV}[u^\nu] \equiv \sup_h \int \left| \frac{u(z+h) - u(z)}{h} \right| dz \quad (15)$$

is non-increasing with time. Assuming  $u^\nu$  is smooth, we have

$$\text{TV}[u^\nu] = \int \left| \frac{\partial u}{\partial z} \right| dz, \quad (16)$$

$$\frac{d}{dt} \text{TV}[u^\nu] = \frac{d}{dt} \int \left| \frac{\partial u}{\partial z} \right| dz \leq 0. \quad (17)$$

For the scalar hyperbolic conservation law (12), the entropy solution is defined to be  $u(t, z) \equiv \lim_{\nu \rightarrow 0} u^\nu(t, z)$ . When numerically solving Eq. (12) for an entropy solution, it is desirable to adopt an algorithm that preserves the property of non-increasing total variation for the exact entropy solutions [32–34].

If one chooses to, Eq. (13) can be viewed as an extremely simplified version of the two-stream system described by Eqs. (1)–(4) when the two components are cold ( $p_j = 0$ ) and do not interact ( $E = 0$ ), which stripes away all possible hidden free energy and total variation cannot grow.

Obviously, the properties of non-increasing total variation at finite viscosity does not hold for the general two-stream system governed by Eqs. (1)–(4). As we have shown, in certain certain parameter regimes, the linear dynamics of the system, which is otherwise stable, can be destabilized by finite viscosity via explicit PT-symmetry breaking. For these cases, at the equilibrium  $(n_{10}, n_{20}, v_{10}, v_{20}, p_{10}, p_{20})$ , when the initial perturbation is small, the dynamics is dominated by the linear eigenmodes for a short time at  $0 < t < \delta$ . If the initial perturbation takes the form of the an unstable eigenmode with a given  $k$  and  $\omega = \omega_R + i\omega_I$  ( $\omega_I > 0$ ), then we have

$$\frac{d}{dt} \int \left| \frac{\partial E}{\partial z} \right| dz \sim \omega_I e^{\omega_I t} \int |kE| dz > 0, \quad (18)$$

i.e., the total variation of the electric field  $E$  increases with time. The same result holds for all other field variable as well. Of course, at zero viscosity, the two-stream interaction can be physically unstable via spontaneous PT-symmetry breaking, resulting in total variation growth as well. The complexity of the dynamics in plasmas with different charge components needs to be considered when designing or selecting algorithms for numerical solutions.

This research was supported by the U.S. Department of Energy (DE-AC02-09CH11466).

---

\* [hongqin@princeton.edu](mailto:hongqin@princeton.edu)

† [dorland@pppl.gov](mailto:dorland@pppl.gov)

‡ [ben.israeli@weizmann.ac.il](mailto:ben.israeli@weizmann.ac.il)

- [1] C. S. Kueny and P. J. Morrison, *Physics of Plasmas* **2**, 1926 (1995).
- [2] H. Qin, R. C. Davidson, and W. W. Lee, *Physical Review Special Topics - Accelerators and Beams* **3**, 084401 (2000).
- [3] R. C. Davidson and H. Qin, *Physics of Intense Charged Particle Beams in High Energy Accelerators* (Imperial College Press and World Scientific, Singapore, 2001).
- [4] F. Zimmermann, *Physical Review Special Topics - Accelerators and Beams* **7**, 124801 (2004).
- [5] C. N. Lashmore-Davies, *Physics of Plasmas* **14**, 092101 (2007).
- [6] P. J. Morrison and G. I. Hagstrom, in *Nonlinear Physical Systems*, edited by O. N. Kriillov and D. E. Pelinovsky (Wiley, 2014).
- [7] H. Qin and R. C. Davidson, *Physics of Plasmas* **21**, 064505 (2014).
- [8] R. Zhang, H. Qin, R. C. Davidson, J. Liu, and J. Xiao, *Physics of Plasmas* **23**, 072111 (2016).
- [9] B. Y. Israeli, A. Bhattacharjee, and H. Qin, *Resonant instabilities mediated by drag and electrostatic interactions in laboratory and astrophysical dusty plasmas* (2023), arXiv:2303.13640 [physics.plasm-ph].
- [10] V. I. Arnold, *Mathematical Methods of Classical Mechanics* (Springer-Verlag, New York, 1989).
- [11] M. de Gosson, *Symplectic Geometry and Quantum Mechanics* (Birkhäuser Verlag, Basel, 2006).
- [12] P. A. Dirac, *Proceedings of the Royal Society of London. Series A. Mathematical and Physical Sciences* **180**, 1 (1942).
- [13] W. Pauli, *Reviews of Modern Physics* **15**, 175 (1943).

- [14] M. Krein, Doklady Akad. Nauk. SSSR N.S. **73**, 445 (1950).
- [15] I. M. Gel'fand and V. B. Lidskii, Uspekhi Mat. Nauk **10**, 3 (1955).
- [16] T. Lee and G. Wick, Nuclear Physics B **9**, 209 (1969).
- [17] V. Yakubovich and V. Starzhinskii, *Linear Differential Equations with Periodic Coefficients*, Vol. I (Wiley, New York, 1975).
- [18] C. M. Bender and S. Boettcher, Physical Review Letters **80**, 5243 (1998).
- [19] C. M. Bender, Reports on Progress in Physics **70**, 947 (2007).
- [20] C. M. Bender, D. C. Brody, H. F. Jones, and B. K. Meister, Physical Review Letters **98**, 040403 (2007).
- [21] C. M. Bender and P. D. Mannheim, Physics Letters A **374**, 1616 (2010).
- [22] A. Felski, C. M. Bender, S. Klevansky, and S. Sarkar, Physical Review D **104**, 085011 (2021).
- [23] C. M. Bender, M. Gianfreda, and S. Klevansky, Physical Review A **90**, 022114 (2014).
- [24] R. Zhang, H. Qin, and J. Xiao, Journal of Mathematical Physics **61**, 012101 (2020).
- [25] H. Qin, R. Zhang, A. S. Glasser, and J. Xiao, Physics of Plasmas **26**, 032102 (2019).
- [26] Y. Fu and H. Qin, New Journal of Physics **22**, 083040 (2020).
- [27] H. Qin, Y. Fu, A. S. Glasser, and A. Yahalom, Physical Review E **104**, 015215 (2021).
- [28] C. M. Bender, (2019), private communication.
- [29] O. N. Kirillov, Philosophical Transactions of The Royal Society A **371**, 20120051 (2013).
- [30] O. N. Kirillov, *Nonconservative stability problems of modern physics*, Studies in Mathematical Physics, Vol. 14 (Walter de Gruyter, 2013).
- [31] C.-W. Shu, Numerical methods for hyperbolic conservation laws (2006), Lecture Notes, Brown University.
- [32] A. Harten, Journal of Computational Physics **49**, 357 (1983).
- [33] H. Yee, R. Warming, and A. Harten, Journal of Computational Physics **57**, 327 (1985).
- [34] B. Cockburn and C.-W. Shu, Mathematics of Computation **52**, 411 (1989).